

# SIMULATION-BASED PERFORMANCE ANALYSIS OF IMPREGNATED WOOD WITH PHASE CHANGE MATERIAL FOR ENERGY EFFICIENT TIMBER STRUCTURES

Jakub GRZYBEK<sup>1,2</sup>      Philipp MEFFERT<sup>1</sup>  
Alexander PETUTSCHNIGG<sup>1,3</sup>      Thomas SCHNABEL<sup>1,4</sup>

**Abstract:** *Organic phase change materials (PCMs) offer a promising approach to improving the energy efficiency and sustainability of buildings. Impregnating wood with PCMs presents the opportunity for its application in building construction to reduce energy consumption for heating and cooling of indoor spaces. In this study, the process of solid wood impregnation with PCMs was conducted, along with the characterisation of their thermal properties. To define an optimal melting point and quantity to be incorporated into test cubes exposed outdoors for long term in Kuchl (Austria), a digital model was used to simulate beech and spruce that were impregnated with PCMs featuring two differing melting points. The results show that incorporating PCM into walls and floor can potentially reduce summer overheating by up to 48%. This effect is achieved using a building design that includes wood impregnated with PCM with a lower melting point of around 21°C. However, the building design and use of the employed PCMs do not reduce energy consumption for heating during winter. The results show that the performance is strongly dependent on the melting point of the PCM and its quantity in the building. These findings contribute to improving the design of the experimental test cube with impregnated wood and highlight the challenges.*

**Key words:** *thermal energy storage, building performance, energy simulation, wood modification, bio-based materials.*

---

<sup>1</sup> Department of Green Engineering and Circular Design, Salzburg University of Applied Sciences, Markt 136a, 5431 Kuchl, Austria;

<sup>2</sup> Faculty of Forestry and Wood Technology, Department of Wood Science and Technology, Mendel University in Brno, Brno, Czech Republic;

<sup>3</sup> Department of Material Sciences and Process Engineering, University of Natural Resources and Life Sciences (BOKU), Konrad Lorenz-Straße 24, 3340 Tulln, Austria;

<sup>4</sup> Faculty for Design of Furniture and Wood Engineering, Transilvania University of Brasov, Brasov, Romania;  
Correspondence: Jakub Grzybek; email: [jakub.grzybek@fh-salzburg.ac.at](mailto:jakub.grzybek@fh-salzburg.ac.at).

## 1. Introduction

In the European Union, buildings contribute to 40% of energy consumption and 36% of greenhouse gas emissions, underlining the key role that improving energy efficiency in buildings plays in achieving the carbon neutrality target set by the European Green Deal for 2050 [10]. The energy consumption for space cooling in both the residential and commercial sectors is mainly driven by increased comfort demands and the widespread introduction of air conditioning systems in European countries [17]. This trend is predicted to continue in the future, with advancements in technology, population growth, and increased expectations for indoor comfort.

One potential solution for countering the rising energy demands for heating and cooling is through using phase change materials (PCMs) within building structures [2]. PCMs have the capability to improve thermal inertia, thereby enhancing overall energy performance. Combining PCMs in building structures is an effective technique for mitigating summer overheating and reducing indoor energy consumption for heating and cooling [10].

Latent heat is the energy that a substance either absorbs or releases when it undergoes a transition from one phase to another. Typically, the latent heat is much higher than the sensible heat. During this phase transition, the temperature remains constant [16]. There are three types of phase changes: solid-solid, solid-liquid, and liquid-gas. Among these, the solid-liquid phase transition is particularly favoured in thermal energy storage (TES) applications because of its

capability to store significant amounts of heat whilst causing minimal changes in volume. TES can be employed in building structures as passive systems to buffer peak heating or cooling demand, or in active systems linked to heating, ventilation and air conditioning, and domestic hot water systems [13] to directly reduce energy consumption [16].

Impregnation of PCMs into wood has received attention in recent years because of the excellent properties of wood as a construction material, such as its mechanical resilience, low thermal conductivity, sustainability, and low density (from 300 to 900 kg/m<sup>3</sup> in Europe) [6, 7, 21]. Due to the porosity of wood, PCMs possess the potential to be incorporated into wood, thereby increasing the thermal mass of wooden structures and positively reducing the energy demand of the building for indoor temperature control [20].

Fatty acids are a suitable option for incorporation into wood due to their natural origin and good compatibility with wood [1, 23]. Previous researches have investigated a range of impregnation parameters [3, 11], various wood species [12, 18, 24], multiple bio-based phase change materials [15, 19], and methods to enhance the composite's performance, such as microencapsulation for leakage prevention [5]. Such impregnated wood is a promising approach to be implemented in building structure in passive or active applications.

The aim of the study is to comprehensively analyse the material properties of wood impregnated with PCM, which could be used as a passive system in lightweight timber construction as cladding for interior walls and floors.

The goal is to enhance indoor thermal comfort in the test cubes by addressing two critical aspects: decreasing overheating in summer and conserving heating energy in winter. To achieve this, the optimal melting temperature and amount of PCMs will be determined and applied to test cubes, which will then be exposed to long-term outdoor conditions. In the initial phase, the wood, specifically beech and spruce sapwood, was impregnated and characterised to provide the material properties that can be implemented in the dynamic simulation software. In the following step, the model validation was carried out using an experimental test cube located in Kuchl, Austria. Subsequently, a validated model was used to perform a series of simulations with a PCM layer of impregnated wood on the walls and floor facing the interior of the simulated test cube.

## 2. Materials and Methods

### 2.1. Materials

Capric acid (98%, Sigma-Aldrich, USA), palmitic acid (98%, Thermo Scientific, USA), and stearic acid (97%, Acros Organics, Belgium) were used in the study. Norway spruce sapwood (*Picea abies* L.;  $\rho=470\text{kg/m}^3$ ) and European beech (*Fagus sylvatica* L.;  $\rho=759\text{kg/m}^3$ ) devoid of visible defects (such as knots or cracks) were selected for the impregnation. The dimensions of the samples used for impregnation were 80x80x20 mm. Before impregnation, the wood specimens were conditioned (at 23°C and 65% RH) and had a moisture content of approximately 12%.

## 2.2. Methods

### 2.2.1. Impregnation Process of the Wood

A ternary eutectic mixture composed of saturated fatty acids was formulated for the impregnation of Beech. This mixture consisted of 80% capric acid, 10% stearic acid, and 10% palmitic acid by weight (PCM low). In the case of Spruce impregnation, a eutectic mixture comprising 83% capric acid and 17% stearic acid (PCM high) was employed. The pre-weighed fatty acids were heated until they reached a liquid state and mixed thoroughly. To ensure homogeneity, the mixture underwent a cyclic process of freezing at 0°C followed by melting at 60°C, repeated thrice. The impregnation procedure took place within an autoclave, starting with a 15-minute vacuum at 30 kPa. Subsequently, the valve was opened, enabling the liquid mixture to access the impregnation chamber while concurrently elevating the pressure to 600 kPa, maintained for 1 hour. To ensure low viscosity of the impregnating solution, the temperature in the chamber was kept at 40°C throughout the impregnation [11]. After removing the specimens from the autoclave, they were transferred to oven at a 100°C for 3 hours. Excess PCM was then removed using paper, followed by recording of the specimen's weight.

The weight percentage gain (WPG) was determined by dividing the difference between the initial and final weights of the specimens by their initial weight after equilibrium was reached at 23°C and 65% RH. To evaluate the effectiveness of the impregnation process, the maximum theoretical mass of PCM that the wood could absorb was calculated. This calculation followed the method outlined by Hartig et al. [12], considering an

estimated PCM density of  $980 \text{ kg/m}^3$  (according to Duquesne et al. [9]), along with a cell wall density of  $1500 \text{ kg/m}^3$ .

### 2.2.2. Characterisation of Thermal Properties of Wood

Differential scanning calorimetry (Mettler-Toledo DSC3) under a nitrogen atmosphere was used to determine the thermal properties such as latent heat and to determine the melting and solidification points of the impregnated wood specimens. Samples of mass 20–30 mg were placed in enclosed aluminium crucible pans. The differential scanning calorimetry (DSC) tests were taken between  $0^\circ\text{C}$  and  $40^\circ\text{C}$  at a heating and cooling rate of  $2^\circ\text{C}/\text{min}$  [18]. The heating–cooling cycle was repeated three times. These results were used to prepare the enthalpy curve used in the simulation software.

### 2.2.3. Design of the Experimental Test Cube

The experimental setup consisted of a 1 cubic meter interior volume, constructed using lightweight wood framing which stands on hollow substructure at a height of 70 cm, as illustrated in Figure 1. The experimental test cube (Figure 2) was located in Kuchl – Austria ( $47.63^\circ \text{ N}$ ,  $13.15^\circ \text{ E}$ ) on the university campus. The walls and floor were insulated with 100 mm thick wooden fibre panels, while the top had 200 mm of the same insulation material. The inner wall was clad with 18 mm thick OSB board and the outer wall with 6 mm white-painted softwood plywood. The U-values of the walls and roof are  $0.3271 \text{ W/m}^2\text{K}$  and  $0.1748 \text{ W/m}^2\text{K}$ , respectively. A double-glazed (U-value of  $1.1 \text{ W/m}^2\text{K}$ ) window with dimensions 20 x 80 cm was installed on the south-eastern wall.

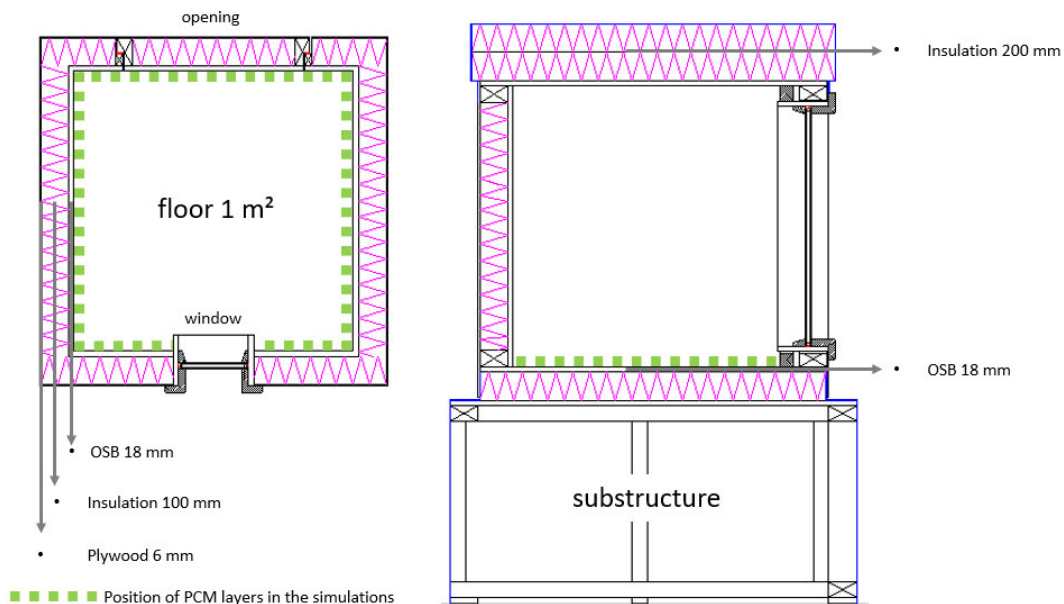


Fig. 1. Plan view (left) and side elevation (right) of the test cube which was placed in Austria used to validate numerical simulations

The experimental test cube was equipped with a 100 W electric heater (RS PRO Enclosure Heater, UK), alongside two fans (Noctua, Austria) with adjustable speeds for controlling inlet and outlet airflow. Temperature sensors with accuracy  $\pm 0.5^{\circ}\text{C}$  (DS18B20, Maxim, U.S.A.) were positioned on the wall and floor surfaces, as well as within the first internal layer and in the centre of indoor space to measure the air temperature and relative air humidity with accuracy  $\pm 0.3^{\circ}\text{C}$  and RH

$\pm 2\%$  (AHT2x, Asair, China). The sensors were shielded from direct sunlight exposure. Data were collected every 90 seconds and the average value in 5-minute intervals was afterwards calculated. Throughout the experiment, the heater with PID controller maintained an internal temperature of 20 degrees Celsius, and no cooling device was employed. The air exchange rate was set at  $1\text{ m}^3/\text{h}$ , equivalent to 1 air changes per hour (ACH).

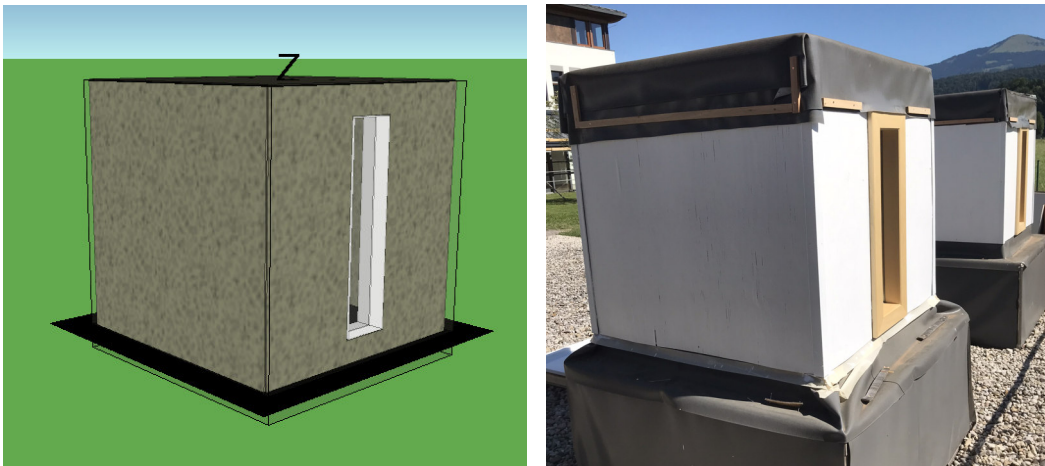


Fig. 2. *Visualisation of simulated test cube in the IDA ICE software (left picture) and experimental test cubes located in Kuchl, Austria (right picture)*

#### 2.2.4. Dynamic Building Performance Simulation – Validation with Experimental Test Cube

To validate the accuracy of the computer simulations, a 2-month period spanning from March to April 2023 was selected, aligning with real-world conditions. Computer simulations were conducted using IDA ICE (EQUA Simulations). The simulation software was configured to replicate parameters from the experimental test cube, encompassing factors such as geographical location,

climate data derived from weather station located in Kuchl (including solar radiation, air temperature, wind speed, and orientation), experimental cube structural details, ventilation settings, and heater specifications. Output in the IDA ICE software of the simulated data were hourly values.

The uncertainty indices used in this study are: normalized mean bias error (NMBE) Equation (1), root mean square (RMSE), and coefficient of variation of the root mean square error (CV RMSE) Equation (2) as suggested by ASHRAE 14

[4, 8, 22]. Where  $s_i$  the simulation predicted datum,  $m_i$  the measured value, and  $n$  the number of measured data points.

The Equations used to calculate *NMBE* (1) and *CV RMSE* (2):

$$NMBE = \frac{\sum_{i=1}^n (m_i - s_i)}{n} \cdot 100 [\%] \quad (1)$$

$$CVRMSE = \frac{\sqrt{\frac{\sum_{i=1}^n (m_i - s_i)^2}{n}}}{\bar{m}} \quad (2)$$

### 2.2.5. One Year Simulation of Test Cube Utilizing Wood Impregnated with PCM

Employing the validated model, simulations were conducted over a span of one year to ascertain the optimal properties of PCM-impregnated wood. Attention was given to determining its melting point and the more suitable quantity for constructing experimental test cubes with PCM. The simulations were based on the validated model, which excluded the PCM impregnated wood. Following these validation simulations, the PCM-impregnated wood was introduced into the simulation software and applied to the walls and floor facing the interior of the virtual test cube. This investigation involved the selection of two distinct PCM compositions, each with varying melting points: Beech impregnated with PCM with a lower melting point (PCM low), and Spruce sapwood impregnated with PCM with a higher melting point (PCM high). Furthermore, for the purposes of the simulations, the data for spruce impregnated with lower melting point and

beech impregnated with higher melting point PCM were generated on the basis of the experimental DSC data, by equivalent substitutions of the amount of PCM that can be hosted by these wood species. Due to its structure, beech can host less PCM than spruce, which affects the total thermal energy that can be stored per volume.

For the simulation process, historical climate data from the year 2022 were utilised. This data were sourced from the IDA ICE database and originated from the Salzburg Airport, located 25 km north of the Kuchl campus where the physical test cube is situated.

The IDA ICE software allows for dynamic simulations involving PCM with distinct melting and solidification temperature properties having flexibility to define these parameters. To accurately represent the behaviour of Beech and Spruce wood impregnated with PCM, a total of 18 specific values, determined through differential scanning calorimetry (DSC) analysis, were incorporated into the material properties. Furthermore, in the simulation software during the period from 1 October to 30 April, the electric heater with a power of 100 W was set at a temperature of 20°C. Simultaneously, the ventilation system operated consistently at a set value of 1 ACH throughout the entire day. In contrast, for the warmer months spanning from 1 May to 30 September, the heater was set at a temperature of 16°C. Ventilation occurred solely during the night-time hours, from 8 pm to 6 am, utilising a rate of 4 ACH. Between 6 am and 8 pm, the ventilation was deactivated to prevent the influx of warm external air into the cube.

### 3. Results and Discussion

#### 3.1. Impregnation Process of the Wood

The outcomes of the impregnation process, presented in Table 1, demonstrate that the weight percentage gain (WPG) of the samples was consistently high for both types of wood. Notably, beech exhibited a lower WPG (37.1%) compared to spruce sapwood (124.1%), which was already presented by Grzybek et al. [11]. Both specimens achieved similar densities after impregnation. Hartig et al. [12] and Nazari et al. [18] showed that the absorption of PCM into wood is influenced by

impregnation parameters such as time, pressure, and PCM viscosity. Furthermore, because of the facility with which PCM penetrates the wood during impregnation, it also tends to leak out of the wood once it has reached a liquid state. Because spruce wood has lower initial density than beech and therefore more free capacities, the specimens can accommodate approximately 55.4% PCM of the total mass, whereas beech specimens hold around 29.9%. Consequently, impregnated spruce is capable of storing more thermal energy, despite occupying smaller volumes.

*Results of the impregnation process of wood with phase change material* Table 1

Specimens	Density [kg/m <sup>3</sup> ]	WPG [%]	Density after impregnation [kg/m <sup>3</sup> ]	Retention [kg/m <sup>3</sup> ]	% PCM in wood [%]
Beech	759.3 (8.8)	37.1 (1.1)	1042.9 (5.9)	322.3 (7.2)	29.9
Spruce	469.5 (12.4)	124.1 (3.5)	1044.7 (2.5)	578.5 (6.8)	55.4

#### 3.2. Characterisation of Thermal Properties of Wood

The simplified enthalpy profiles of both specimens namely spruce and beech, impregnated with PCM, are illustrated in Figure 3. These profiles were derived from differential scanning calorimetry (DSC) analyses, and simplified to fit the input data format of the simulation software - the IDA ICE.

DSC is a sensitive instrument, necessitating small sample sizes (typically 5-40 mg). This sensitivity poses challenges when dealing with heterogeneous samples as PCM incorporated into wood. However, it allows for coarse determination of heat capacity, latent heat, and the melting and solidification points. These parameters are required in

defining material properties for subsequent computer simulations of the test cubes. The outcomes reveal that the melting point for spruce is approximately 27.5°C with latent heat of approximately 80 J/g, while for beech, it is around 21°C and latent heat of about 45 J/g. Additionally, the PCM within spruce starts solidification at approximately 25.5°C, contrasting with beech at 19.5°C. This discrepancy arises from the utilisation of two various PCM types during the impregnation process for spruce and beech, respectively. For the PCM to realise its full potential in a wood matrix, external temperatures must fluctuate above and below the melting and solidifying points. In addition, as a simplification for the purpose of the simulations, the heat

capacity of both wood samples was defined to be equal to  $2 \text{ J/g}\cdot\text{K}$ .

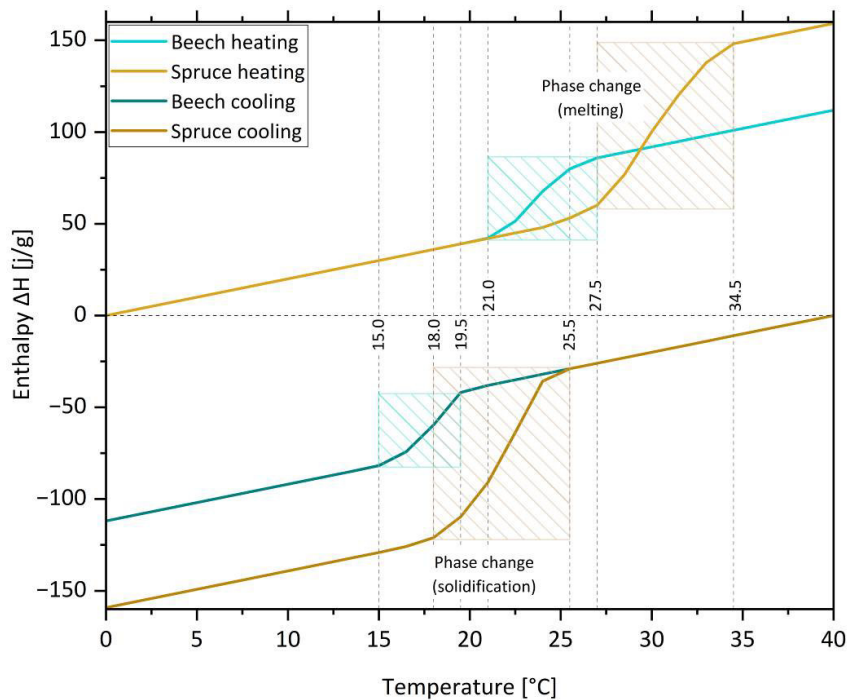


Fig. 3. Simplified enthalpy of wood impregnated with PCM based on DSC measurement used for input of material properties in IDA ICE

### 3.3. Dynamic Building Performance Simulation – Validation with Experimental Test Cube

As illustrated in Figure 4 the comparison between the experimental measurements and the simulated data is shown. To ensure the accuracy of validation, several key metrics were calculated, as outlined by Coakley et al. in 2011 [8]. These metrics include the root mean square error (RMSE), the normalized bias error (NBME), and the coefficient of variation (CV(RMSE)). In the context of indoor temperatures, the calculated RMSE was  $0.7^{\circ}\text{C}$ , with a corresponding NBME of -

1.28%, and a CV(RMSE) of 3.33%. In terms of heater power consumption, the RMSE measured  $6.09 \text{ W}$ , accompanied by an NBME of  $-20.85\%$ , and a CV(RMSE) of 55.65%. If NBME is close to zero, it indicates a small bias between observed and predicted values. Moreover, a negative value means that the model over predicts measured data [22]. According to the ASHRAE Guideline 14 [4], to validate the computer simulation model, accuracy should exhibit within  $\pm 10\%$  for NBME and 30% for CV(RMSE), relative to hourly measured data. The comparison between the simulation and experimental data for indoor temperature indicates a high



degree of similarity and closely aligned trends, meeting the criteria set for validation by ASHRAE. Thus, the model can be considered as validated for indoor temperature predictions.

However, the same trend does not apply to electric heater power consumption, as the determined values exceed the stipulated guideline values. Although there are similarities in appearance and alignment between the heating power consumption trends observed in

simulations and experimental data, the level of precision is still inadequate. This inadequacy indicates that additional refinements are necessary for the simulation model to improve its accuracy. This discrepancy becomes evident when considering total electricity usage. During the tested period, the experimental setup consumed 15.5 kWh, while the simulated cube consumed 18.73 kWh over the same time, which is 20.8% more.



Fig. 4. Comparison of indoor air temperature (top graph) and electric heater current (bottom graph) between experimental test cubes and simulated cube in April and May 2023

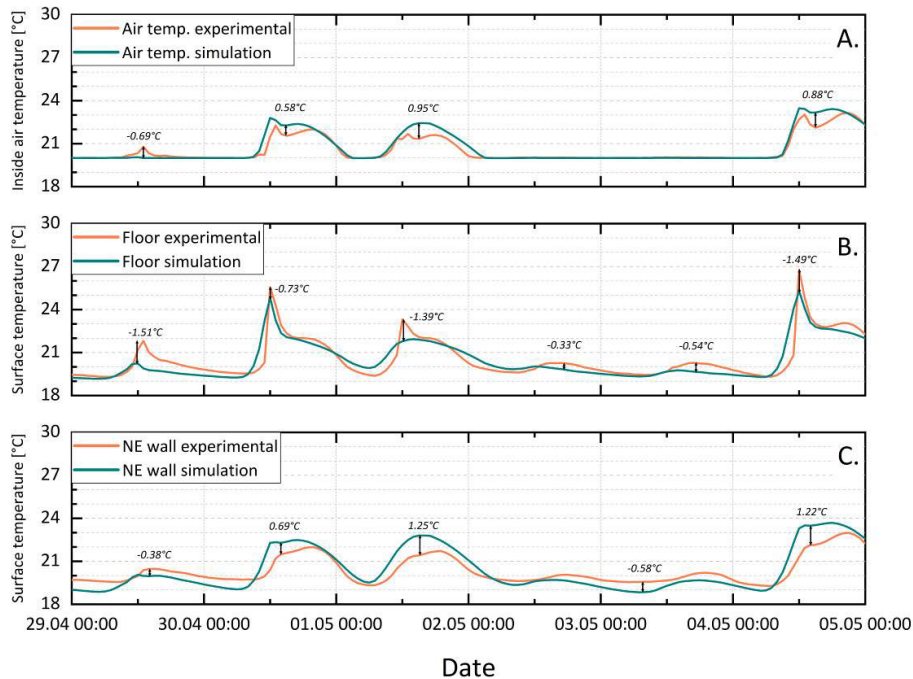


Fig. 5. Detailed visualisation of experimental data and simulated data between 29.04 and 05.05 2023: a. indoor air temperature: b. surface temperature of floor: c. surface temperature of inner wall surface exposed north-east

Figure 5 illustrates the detailed variations in air temperature (a.), as well as the temperatures on the inner surfaces of the floor (b.), and the north-east wall (c.), in comparison to the simulated values and experimental data. The comparison reveals that while the simulated data generally follow a similar trend to the experimental data, there are instances of shifted temperature increases or prolonged periods, leading to a deviation of approximately one hour. This effect is particularly evident in the floor surface temperature which can be caused by the fact that in the experimental setup, the sensor is positioned centrally, making it more susceptible to direct solar radiation. In contrast, the simulated data account for

temperature readings collected from the entire surface area of the test cube.

During the period from 2.05 to 4.05, the indoor temperature remained constant at 20°C due to low solar radiation and low outdoor temperature. However, the surface temperatures exhibited fluctuations, displaying slight increases during daylight hours. Notably, even within the confined 1m<sup>3</sup> test cube, the distribution of temperature is made in dependence of the sensor placement.

### 3.4. One Year Simulation of Test Cube Utilising Wood Impregnated with PCM

Using the validated model presented in the previous section, a numerical study was carried out to optimise the designs for

applying PCM layers and to investigate the amount of PCM required to be applied in test cubes located in Kuchl (Austria), in order to improve the indoor thermal environment, reduce the energy required for heating, and reduce summer overheating. The simulations were performed based on the validated model of the test cubes which included an extra layer of the PCM impregnated wood of beech and spruce with various thickness on the inner walls and the floor.

As showed in Table 2, the amount of PCM per square meter is 6.44 kg/m<sup>2</sup> for impregnated beech and 11.57 for impregnated spruce with PCM. In other similar numerical or experimental studies around the world, the amount of PCM in building structure varies from 0.9 kg/m<sup>2</sup> up to 11 kg/m<sup>2</sup> [14].

*Table 2*  
*Total weight of PCM and PCM by surface area in the impregnated wood used in the simulations of experimental test cube*

Specimens	PCM impregnated wood layer (thickness 2 cm)	
	[kg/m <sup>2</sup> ]	total mass of PCM [kg]
Beech	6.44	31.17
Spruce	11.57	55.99

Figure 6 illustrates the maximal daily indoor temperatures during the warmer months. Clearly evident from the visualisation is the impact of PCM integration within the test cubes. These cubes exhibit a reduction in the number of days where temperatures exceed 25°C and a remarkable stability in temperature fluctuations, maintaining a more consistent thermal profile.

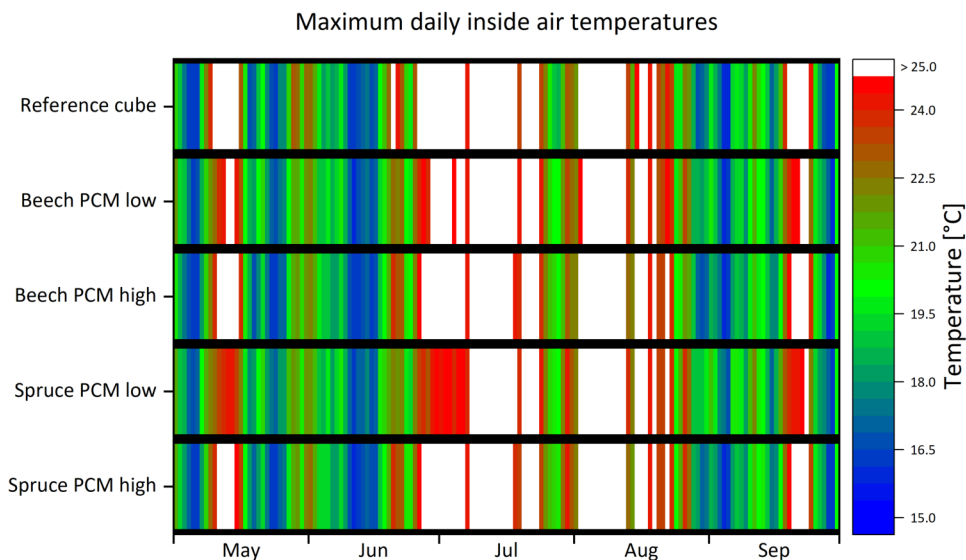


*Fig. 6. Heat map of daily maximum temperature between May and September in simulated test cubes*

Additional insights are shown in Table 3, which presents data on energy consumption and the occurrences of days surpassing 25°C over a whole year. Notably, an increase in the amount of PCM within the test cubes leads to a decrease in the number of hours or days exceeding 25°C. This effect is prominently

demonstrated by the test cube equipped with spruce wood incorporated with PCM with lower melting point, showing a reduction of 48.12% when compared to the reference test cube. In contrast, the test cube with spruce and higher melting point PCM demonstrates a reduction of 16.55%.

Table 3

*Summary of the occurrence of indoor air temperature over 25°C and electricity usage for heater in simulated test cubes over a year*

Cube						
		Reference	Beech PCM low	Beech PCM high	Spruce PCM low	Spruce PCM high
Temperatures over 25°C – time of occurrence	in days	54	39	45	28	46
	in hours	719	501	619	373	600
Reduction	%	-	30.32	13.91	48.12	16.55
Electricity consumption for heating [kWh]						
Months	Jan	36.3	36.8	36.8	36.8	36.8
	Feb	27.3	27.6	27.7	27.7	27.7
	Mar	22.8	23.1	23.0	23.2	23.0
	Apr	13.9	14.3	14.0	14.4	14.1
	May	1.6	0.5	1.1	0.2	1.0
	Jun	0.6	0.5	0.5	0.4	0.5
	Jul	0.0	0.0	0.0	0.0	0.0
	Aug	0.3	0.0	0.1	0.0	0.0
	Sep	2.0	1.1	1.7	0.3	1.6
	Oct	14.6	15.1	14.9	14.9	15.0
	Nov	26.1	26.4	26.3	26.4	26.3
	Dec	33.7	34.0	34.1	34.1	34.1
<b>Total</b>	-	<b>179.2</b>	<b>179.4</b>	<b>180.2</b>	<b>178.4</b>	<b>180.1</b>

This reduction in temperatures surpassing 25°C can be attributed to the specific characteristics of the PCM integrated into the respective cubes. The PCM low with lower melting point initiates its melting phase at 21.0°C, while the PCM high with higher melting point initiates its

phase change at 27.5°C. This difference in phase change temperatures directly contributes to the overall better thermal performance in reducing heat in the test cubes with PCM low during the warm months of the year.

Figure 7 illustrates the temperature profile of the warmest internal surface, namely the floor, within the reference cube. The figure shows that temperatures above the melting point of the PCM low (21°C) start to occur in the second half of April and last until the first half of October. It should be noted that temperatures above 27°C occur mainly in July and around July with single occurrences in May. These temperature patterns correspond well to the lower melting point of the PCM low. Similar results from other researchers suggested

that the PCM material used with a melting point of 21.6°C was effective in reducing high internal temperatures even in regions with moderate climate zones [14]. However, a critical limitation occurs when temperatures continuously exceed the 21°C threshold for a prolonged period of time over several days. This elevated temperature for a long period of time prevents the wood impregnated with PCM from reverting to its solid state, thereby hindering the PCM from being fully utilised.

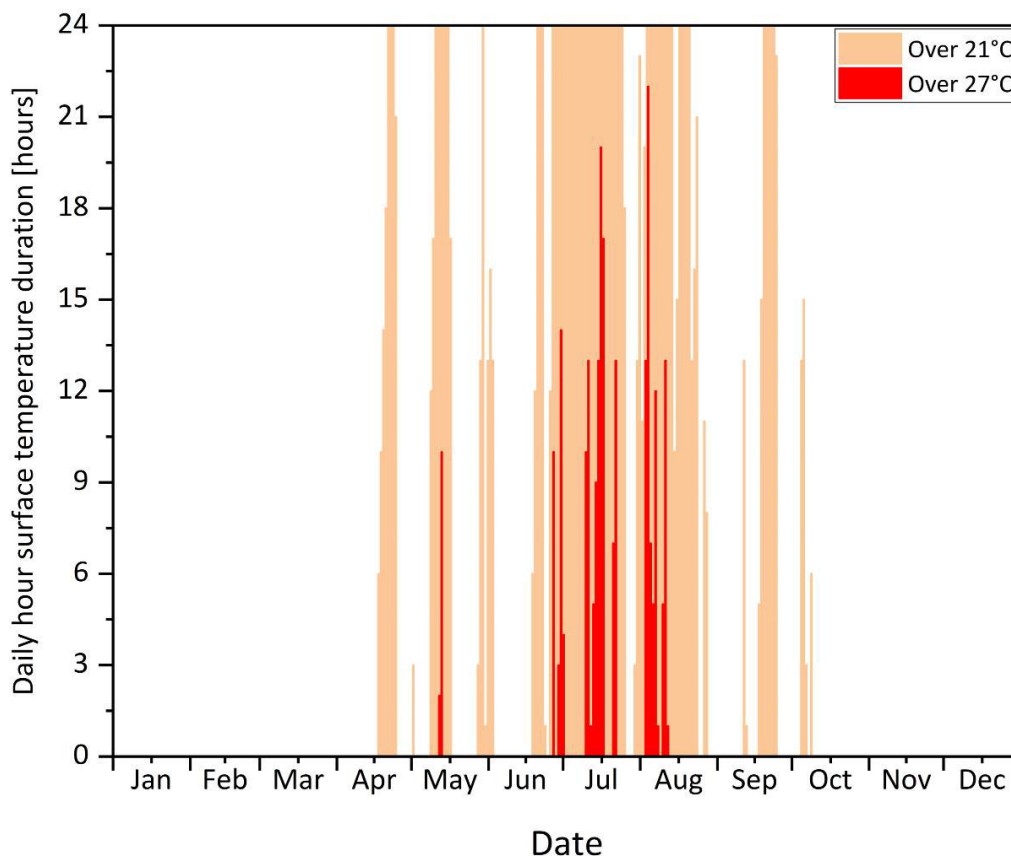


Fig. 7. Occurrence in hours of the surface temperature of the floor in the simulated reference cube

The PCMs integrated into the building design demonstrate excellent performance in reducing maximum temperatures. A detailed analysis of the hottest days recorded between 14 July and 18 July (as shown in Figure 8) reveals a clear contrast between the indoor air temperatures within the reference cube

and those with incorporated PCM. The PCM low performs visibly better in terms of reducing the peak temperatures. Moreover, increasing the amount of PCM by incorporating PCM low in spruce shows the greatest reduction. On the hottest day, this reduction reaches around 1.8°C for both simulated cubes with PCM low.

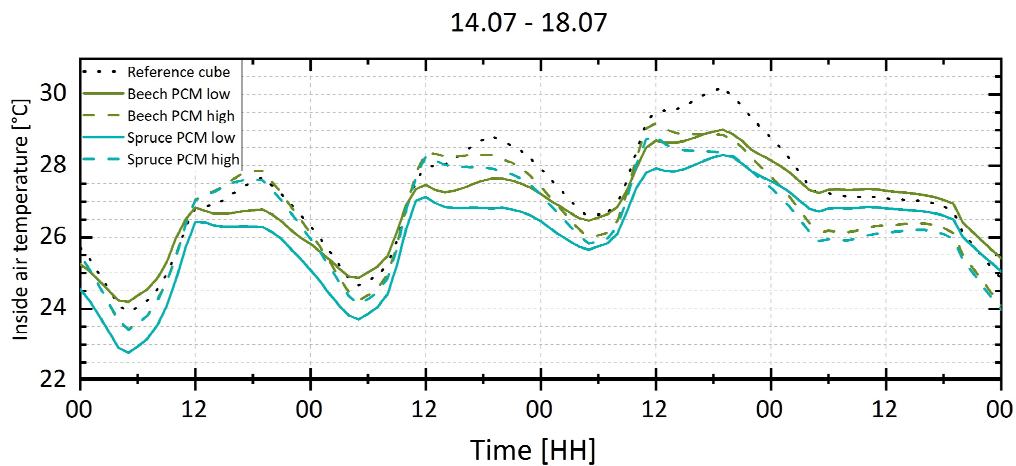


Fig. 8. Detailed visualisation of maximal indoor air temperature of simulated test cubes with PCM impregnated beech and spruce between 14.07 and 18.07

As previously mentioned, the prolonged period of high outdoor temperatures and continued heat, which prevents the test cubes from cooling down, may have a negative effect on indoor temperatures. This trend can be seen in Figure 9, which includes the data for the interval after a series of warm days. The presence of PCMs intensifies the internal heat due to their ability to accumulate thermal energy. However, this property also extends the duration of cooling. Such an effect could

be advantageous in situations where the temperature fluctuates greatly between day and night. This would allow the PCM-equipped cubes to stabilise the ambient temperature during the night, while limiting heat accumulation during the day. This beneficial behaviour is noticeable on the last two days presented (24.08 - 26.08). For all cubes tested with PCM, the maximum temperatures between 19.08 and 24.08 were consistently higher than for the reference cube.

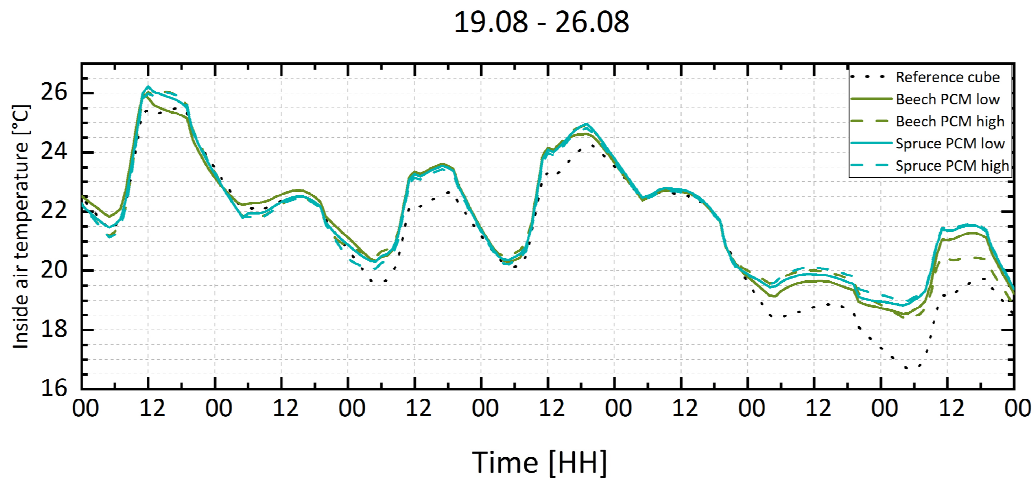


Fig. 9. Detailed visualisation of indoor air temperature of simulated test cubes with PCM impregnated beech and spruce between 19.08 and 26.08

Lastly, the energy consumption of the cubes is assumed for the whole year (Table 3). Although the simulation has not been validated according to ASHRAE, as the simulations overpredict the results, it shows a similar course to the experimental part. The energy consumption values may be compared, but the values should not be taken as real and are likely to be about 20% too high. The overall trend over the year clearly shows that all the cubes consume almost the same amount of energy for the electric heater. However, as less external energy is provided to melt the PCM (Figure 7), there is no exception to see a beneficial effect on energy reduction during the winter. However, the additional thermal mass does not negatively affect the thermal performance of the house - there is only a slight increase in energy consumption in winter as the amount of PCM used increases. The additional thermal mass attached to the inside of the external wall could act as a conductor for heat transfer. In winter, the heat generated by the heating system inside

the building is transmitted through the additional thermal mass and transferred to the colder external face of the wall. This increases the heat loss through the external wall. However, the extra energy used in winter is recovered in the transition period before and after summer, making the overall total energy consumption for the whole year comparable.

#### 4. Conclusions

In conclusion, this paper presents the results of an experimental investigation of the impregnation of beech and spruce sapwood with bio-based organic phase change materials (PCMs) derived from fatty acids. Furthermore, it includes the validation of a digital model of a test cube and dynamic simulations with PCM impregnated wood layers on the internal walls and floor. The main objective of this study was defining the material properties of PCM to improve the indoor thermal environment, mitigating overheating in summer and reducing heating energy

consumption in winter, by determining the optimum melting temperature and quantity to be applied to the test cubes for long-term exposure under real-world conditions.

Key findings of this investigation are listed below:

- Successful model validation: The digital model of the test cubes demonstrated its effectiveness in performing indoor temperature analysis, validating its reliability for future simulations;
- Winter energy savings: The integration of the proposed PCMs resulted in negligible effects on winter energy savings. This implies that the proposed PCMs and building design may not affect heating energy consumption during colder months;
- Improved summer comfort: Increasing the amount of PCM in the simulated test cube resulted in clear improvements in maintaining indoor temperatures below 25°C during the summer season. The reduction in hours with temperatures above 25°C varied from 13.91% to 48.12%. The higher reduction can be achieved by impregnating spruce, which can host more PCM than beech;
- Importance of melting temperature: The performance of PCM is strongly dependent on the melting temperature of the PCM. The PCM with the lower melting point of around 21°C showed the most favourable results in terms of indoor thermal regulation.

By optimising the amount of PCM and selecting the appropriate melting point of the PCM, benefits can be achieved in reducing summer overheating while maintaining winter energy efficiency. These results contribute to improving the

design and selection of the materials for use in the test cubes that will be exposed outside.

### Acknowledgements

Funding: The study was carried out within the framework of the Smart Energy Systems Research and Innovation Program (ERA-Net E2B2) in the project “Bio-Based Phase Change Materials Integrated into Lignocellulose Matrix for Energy Store in Buildings (BIO-NRG-STORE)”. The authors acknowledge the financial support by Austrian Research Promotion Agency (FFG), project number 879308.

### References

1. Al-Ahmed, A., Jafar Mazumder, M.A., Salhi, B. et al., 2021. Effects of carbon-based fillers on thermal properties of fatty acids and their eutectics as phase change materials used for thermal energy storage: A Review. In: *Journal of Energy Storage*, vol. 35, ID article 102329. DOI: [10.1016/j.est.2021.102329](https://doi.org/10.1016/j.est.2021.102329).
2. Álvarez, S., Cabeza, L.F., Ruiz-Pardo, A. et al., 2013. Building integration of PCM for natural cooling of buildings. In: *Applied Energy*, vol. 109, pp. 514-522. DOI: [10.1016/j.apenergy.2013.01.080](https://doi.org/10.1016/j.apenergy.2013.01.080).
3. Amini, M.H.M., Temiz, A., Hekimoğlu, G. et al., 2022. Properties of Scots pine wood impregnated with capric acid for potential energy-saving building material. In: *Holzforschung*, vol. 76(8), pp. 744-753. DOI: [10.1515/hf-2022-0007](https://doi.org/10.1515/hf-2022-0007).
4. ASHRAE 14, 2002. Guideline 14-2002: Measurement of energy and demand savings. Available at:



- <https://webstore.ansi.org/standards/ashrae/ashraeguideline142002>. Accessed on: October, 2023.
5. Can, A., 2023. Preparation, characterization, and thermal properties of microencapsulated palmitic acid with ethyl cellulose shell as phase change material impregnated wood. In: *Journal of Energy Storage*, vol. 66, ID article 107382. DOI: [10.1016/j.est.2023.107382](https://doi.org/10.1016/j.est.2023.107382).
  6. Can, A., Lee, S.H., Antov, P. et al., 2023. Phase-change-material-impregnated wood for potential energy-saving building materials. In: *Forests*, vol. 14(3), ID article 514. DOI: [10.3390/f14030514](https://doi.org/10.3390/f14030514).
  7. Can, A., Žigon, J., 2022. N-Heptadecane-Impregnated wood as a potential material for energy-saving buildings. In: *Forests*, vol. 13(12), ID article 2137. DOI: [10.3390/f13122137](https://doi.org/10.3390/f13122137).
  8. Coakley, D., Raftery, P., Molloy, P. et al., 2011. Calibration of a detailed BES model to measured data using an evidence-based analytical optimization approach. In: *Proceedings of Building Simulation 2011: 12<sup>th</sup> Conference of International Building Performance Simulation Association*, 14-16 November, Sydney, Australia, pp. 374-381.
  9. Duquesne, M., Mailhé, C., Doppiu, S. et al., 2021. Characterization of fatty acids as biobased organic materials for latent heat storage. In: *Materials*, vol. 14(16), ID article 4707. DOI: [10.3390/ma14164707](https://doi.org/10.3390/ma14164707).
  10. Fetting, C., 2020. The European Green Deal. ESDN Report, November 2020, ESDN Office, Vienna, Austria. Available at: [https://www.google.com/url?sa=t&rc=t=&q=&esrc=s&source=web&cd=&ved=2ahUKEwj\\_6sPt--2CAxUmhf0HHeT2ASEQFnoECA4QAQ&url=https%3A%2F%2Fwww.esdn.eu%2Ffileadmin%2Fpdf%2FConferences%2F2020\\_Berlin%2FESDN\\_Conference\\_2020\\_Report\\_Final.pdf&usq=AOVaw0cRFLyZmG0aR8oiHK8OTW\\_&opi=89978449](https://www.google.com/url?sa=t&rc=t=&q=&esrc=s&source=web&cd=&ved=2ahUKEwj_6sPt--2CAxUmhf0HHeT2ASEQFnoECA4QAQ&url=https%3A%2F%2Fwww.esdn.eu%2Ffileadmin%2Fpdf%2FConferences%2F2020_Berlin%2FESDN_Conference_2020_Report_Final.pdf&usq=AOVaw0cRFLyZmG0aR8oiHK8OTW_&opi=89978449). Accessed on: October, 2023.
  11. Grzybek, J., Paschová, Z., Meffert, P. et al., 2023. Impregnation of Norway spruce with low melting-point binary fatty acid as a phase-change material. In: *Wood Material Science and Engineering*, vol. 18(5), pp. 1755-1764. DOI: [10.1080/17480272.2023.2186266](https://doi.org/10.1080/17480272.2023.2186266).
  12. Hartig, J., Hilker, F., Wehsener, J. et al., 2022. Impregnation of wood with a paraffinic phase change material for increasing heat capacity. In: *Wood Material Science and Engineering*, vol. 18(1) – 10<sup>th</sup> European Conference on Wood Modification\_ECWM\_2020, pp. 19-28. DOI: [10.1080/17480272.2022.2133630](https://doi.org/10.1080/17480272.2022.2133630).
  13. Heier, J., Bales, C., Martin, V., 2015. Combining thermal energy storage with buildings – a review. *Renewable and Sustainable Energy Reviews*, vol. 42, pp. 1305-1325. DOI: [10.1016/j.rser.2014.11.031](https://doi.org/10.1016/j.rser.2014.11.031).
  14. Kuczyński, T., Staszczuk, A., 2023. Experimental study of the thermal behavior of PCM and heavy building envelope structures during summer in a temperate climate. In: *Energy*, vol. 279, ID article 128033. DOI: [10.1016/j.energy.2023.128033](https://doi.org/10.1016/j.energy.2023.128033).
  15. Mathis, D., Blanchet, P., Landry, V. et al., 2018. Impregnation of wood with

- microencapsulated bio-based phase change materials for high thermal mass engineered wood flooring. In: *Applied Sciences*, vol. 8(12), ID article 2696. DOI: [10.3390/app8122696](https://doi.org/10.3390/app8122696).
16. Mehling, H., Cabeza, L.F., 2008. Heat and cold storage with PCM. Springer eBooks. Available at: <https://link.springer.com/book/10.1007/978-3-540-68557-9>. Accessed on: October, 2023.
17. Navarro, L., de Gracia, A., Niall, D. et al., 2016. Thermal energy storage in building integrated thermal systems: A review. Part 2. Integration as passive system. In: *Renewable Energy*, vol. 85, pp. 1334-1356. DOI: [10.1016/j.renene.2015.06.064](https://doi.org/10.1016/j.renene.2015.06.064).
18. Nazari, M., Jebrane, M., Terziev, N. et al. 2022. Solid wood impregnated with a bio-based phase change material for low temperature energy storage in building application. In: *Journal of Thermal Analysis and Calorimetry*, vol. 147(19), pp. 10677-10692. DOI: [10.1007/s10973-022-11285-9](https://doi.org/10.1007/s10973-022-11285-9).
19. Nazari, M., Jebrane, M., Terziev, N., 2021. Multicomponent bio-based fatty acids system as phase change material for low temperature energy storage. In: *Journal of Energy Storage*, vol. 39, ID article 102645. DOI: [10.1016/j.est.2021.102645](https://doi.org/10.1016/j.est.2021.102645).
20. Nazari, M., Jebrane, M., Terziev, N., 2020. Bio-based phase change materials incorporated in lignocellulose matrix for energy storage in buildings – a review. In: *Energies*, vol. 13(12), ID article 3065. DOI: [10.3390/en13123065](https://doi.org/10.3390/en13123065).
21. Palanti, S., Temiz, A., Demirel, G.K. et al., 2022. Bio-based phase change materials for wooden building applications. In: *Forests*, vol. 13(4), ID article 603. DOI: [10.3390/f13040603](https://doi.org/10.3390/f13040603).
22. Ruiz, G.R., Bandera, C.F., 2017. Validation of calibrated energy models: common errors. In: *Energies*, vol. 10(10), ID article 1587. DOI: [10.3390/en10101587](https://doi.org/10.3390/en10101587).
23. Singh, P., Sharma, R.K., Ansu, A.K. et al., 2021. A comprehensive review on development of eutectic organic phase change materials and their composites for low and medium range thermal energy storage applications. In: *Solar Energy Materials and Solar Cells*, vol. 223, ID article 110955. DOI: [10.1016/j.solmat.2020.110955](https://doi.org/10.1016/j.solmat.2020.110955).
24. Temiz, A., Hekimoğlu, G., Demirel, G.K. et al., 2020. Phase change material impregnated wood for passive thermal management of timber buildings. In: *International Journal of Energy Research*, vol. 44(13), pp. 10495-10505. DOI: [10.1002/er.5679](https://doi.org/10.1002/er.5679).